Numerical Modeling of Dislocation-Grain Boundary Interaction and Continuum Mechanics Analyses for Mechanical Properties of Fine Grained Metals

Tetsuya Ohashi[1, a], Ryota Tsugawa[1,b] and Tomotaka Ogasawara[1,c]
[1]Department of Mechanical Systems, Kitami Institute of Technology,
Koencho 165, Kitami, Hokkaido 0908507, Japan
[a]ohashi@newton.mech.kitami-it.ac.jp, [b]tsugar@newton.mech.kitami-it.ac.jp,
[c]ogasa@newton.mech.kitami-it.ac.jp

Keywords: Dislocation dynamics simulation, finite element method, strain gradient, crystal plasticity, dislocation source, grain boundary, stress-strain curves, scale dependency

Abstract. Macroscopic mechanical response of metal polycrystal with mean grain diameter of 0.2 to 5 microns are simulated by a strain gradient crystal plasticity software code which incorporates some phenomenological models for dislocation accumulation and annihilation, as well as dislocation-grain boundary interactions. Obtained results of macroscopic stress-strain relation show significant increase of yield stress and strain hardening ratio for fine grained specimens.

Introduction

It is well known that yield stress and strain hardening property of metal polycrystals change largely with their mean grain diameter, while the theoretical background for the prediction of such scale dependent characteristics is not fully developed. Recently, plastic strain gradient and/or the geometrically necessary (GN) dislocations was introduced into the expressions of plastic flow stress [1] or strain hardening [2] and the scale dependent character was discussed [3, 4]. Effects of grain boundaries to the movement of dislocations was also introduced into the expression of the critical resolved shear stress of slip systems and scale dependence of yield stresses were incorporated into the theory [5]. Now, we are interested in the combined effects of the strain gradient and grain boundary-dislocation interactions.

In this communication, we use GN and SS (statistically stored) dislocations to model the mean free path of moving dislocations and also introduce the effect that the mean free path is limited by the size of individual crystal grains. Tensile deformations of six-grained polycrystal plates are numerically analyzed and scale dependence of yield stresses and strain hardening characteristics are examined.

Critical Resolved Shear Stress with the Effect of Grain Boundaries [5]

Let us assume a cuboidal-shaped single crystal specimen of copper (Fig. 1). Six surfaces of the specimen correspond to grain boundaries, and movement of dislocations is confined to the interior of the specimen. The dimension of the slip plane which is trimmed by four grain boundary planes is $d \times d$ and a dislocation segment of length λ and the magnitude of the Burgers vector $\tilde{b}$ is placed on it. Both ends of the dislocation segment are assumed to be pinned and cannot move. Movement of dislocations is numerically studied by a dislocation dynamics (abbreviated as DD, hereafter) simulation software code [6]. Uniformly distributed shear stress τ is applied to the specimen.

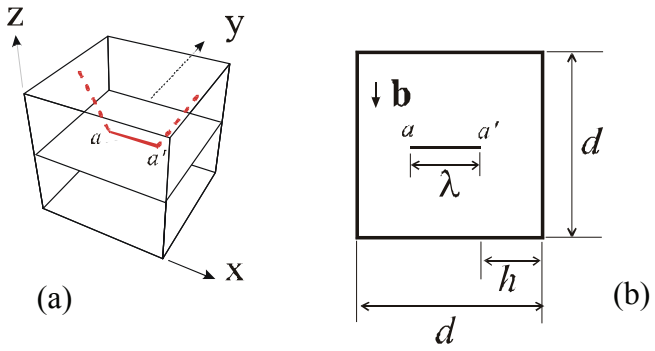

Fig. 1 (a) Cuboidal shaped single crystal specimen employed for the dislocation dynamics simulation. A Frank-Read type dislocation source is placed at the center of the specimen. (b) Dimension of the specimen and the FR source.

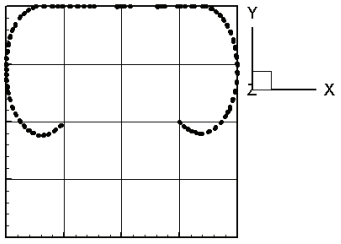

Fig. 2 Stable shape of the dislocation arc emetted from the FR source when $d/\lambda = 2$ and $\tau/\tau_\infty = 1.9$.

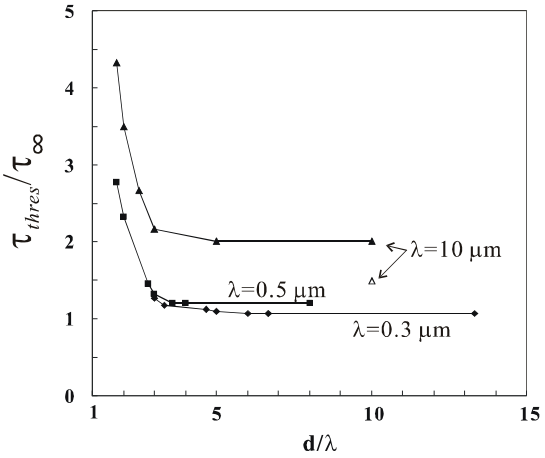

Fig. 3 The minimum shear stress τ_{thres} to emit a closed dislocation loop inside a crystal grain plotted against the ratio of sizes of grain and FR source.

If $d \gg \lambda$, dislocation loop(s) are emitted when $\tau \approx \tau_\infty$, where $\tau_\infty = \mu\tilde{b}/\lambda$. The larger the source length λ is the easier to emit dislocation loops. While, if the source length is close to the grain size, some parts of the dislocation line hit the grain boundary before a closed dislocation loop is formed. Fig. 2 shows the results when $\lambda = 0.5\mu m$, $d = 1\mu m$ and $\tau = 1.9\tau_\infty$. Growth of the dislocation arc stops after it hit grain boundaries and sharply bent. Larger stress is needed to form a closed dislocation loop.

The minimum shear stress τ_{thresh} (critical stress) at which the FR source emits a closed loop is searched by DD simulation for various conditions of grain and FR source sizes. Details of the simulations are described in Ohashi *et al*. [5]. The results obtained are shown in Fig. 3. When the ratio of the grain size to FR source length is sufficiently large ($d/\lambda \gg 3$), the stress ratio $\tau_{thresh}/\tau_\infty$ needed for a FR source to emit a dislocation loop does not depend on the grain size, while in the region $d/\lambda < 3$, the ratio $\tau_{thresh}/\tau_\infty$ rapidly increases with reduction of grain size. This fact, in turn, indicates that when shear stress is gradually applied to a crystal grain with a certain grain diameter, a FR source with length nearly equal to 1/3 of the grain diameter and positioned near the center of the grain emits the first dislocation loop. The minimum shear stress needed to emit a dislocation loop is then given as a function of grain size d by

$$\tau = \beta \frac{\mu \tilde{b}}{(d/3)} = 3\beta \frac{\mu \tilde{b}}{d}, \tag{1}$$

when there are no obstacles to the expansion of a dislocation arc other than grain boundaries. Coefficient β, which is defined by the ratio of the level-off stress and τ_∞, is dependent on the FR source length λ and other factors, but its dependence on λ is weak.

Let us implement the results of the dislocation dynamics simulations into the continuum mechanics-based crystal plasticity theory. Dislocation arc emitted from a dislocation source has to intersect with grown-in dislocations and interact with grain boundary planes also. These process contribute to raise the critical resolved shear stress. If slip resistance by grown-in dislocations or other obstacles play as much of a role as the grain boundaries do, we can simply add these slip resistances to give the extended Bailey-Hirsch type model for the critical resolved shear stress (CRSS):

$$\theta^{(n)} = \theta_0(T) + \sum_{m=1}^{12} \Omega^{(nm)} a \mu \tilde{b} \sqrt{\rho_S^{(m)}} + 3\beta \frac{\mu \tilde{b}}{d}, \tag{2}$$

where $\rho_S{}^{(m)}$ is initially the density of grown-in dislocations and after the onset of slip deformation the density of SS dislocations on slip system *m*.

Models for Dislocation Density Evolution

Accumulation and annihilation of SS dislocations during plastic strain increment is given by the following model [7],

$$d\rho_S^{(n)} = \left(\frac{c}{\tilde{b} L^{(n)}} - \frac{D}{\tilde{b}} \rho_S^{(n)} \right) d\gamma^{(n)}, \tag{3}$$

where, $\gamma^{(n)}$ denotes plastic shear strain on slip system *n*. Numerical factor *c* is the velocity ratio of edge and screw dislocations, *D* the representative length scale for dislocation annihilation, and $L^{(n)}$ the mean free path (abbreviated as MFP, hereafter) of moving dislocations on the slip system *n*. Recently, we introduced a new model [2,8] for the MFP which was given by,

$$L^{(i)} = \frac{c^*}{\sqrt{\sum_j w^{(ij)} \left(\rho_S^{(j)} + \left\| \rho_G^{(j)} \right\| \right)}}. \tag{4}$$

$\left\| \rho_G^{(j)} \right\|$ is the density norm of the GN dislocations on slip system *j* and defined by the following equations,

$$\left\| \rho_G^{(n)} \right\| = \sqrt{(\rho_{G,edge}^{(n)})^2 + (\rho_{G,screw}^{(n)})^2}, \tag{5}$$

$$\rho_{g,edge}^{(n)} = -\frac{1}{\tilde{b}}\frac{\partial \gamma^{(n)}}{\partial \xi^{(n)}},\ \rho_{g,screw}^{(n)} = -\frac{1}{\tilde{b}}\frac{\partial \gamma^{(n)}}{\partial \zeta^{(n)}} \quad . \tag{6}$$

Here, $\xi^{(n)}$ and $\zeta^{(n)}$ denote the crystal coordinates of slip system *n*, respectively. Density components of GN dislocations are evaluated by spatial gradient of plastic shear strain, and so density norm of GNDs $\left\|\rho_G^{(j)}\right\|$ is scale dependent. This fact brings about a scale dependent characteristics in the accumulation of the SS dislocations.

Weight $w^{(ij)}$ determines the contribution of dislocations on the slip system *j* to the MFP of the moving dislocations on the slip system *i*. If we assume $w^{(ij)} = 1$ for $i, j = 1,...12$, Eq. 4 reflects a physical picture that the MFP is given by $c^* \times$(*mean spacing of dislocations accumulated on twelve slip systems*). However, it is not likely that dislocations accumulated on the same slip plane with the moving ones obstruct their movement. Therefore, we assume in this paper that the weight for the dislocations on the same slip plane with the moving ones is zero, while the other components of the weight matrix for forest dislocations are set as 1.

When the size of crystal grains is large enough compared to the average distance of accumulated dislocations, Eq. 4 will be a good approximation of MFP. In the case of fine grained materials such as the materials classes obtained by severe plastic deformations where the average grain diameter is in a few to sub-micron range, dislocations may hit the grain boundary before they interact with accumulated ones. Effect of grain boundaries on the MFP is simply introduced in the following model,

$$L^{(i)} = \mathrm{Min}\left[\frac{c^*}{\sqrt{\sum_j w^{ij}\left(\rho_S^{(j)} + \left\|\rho_G^{(j)}\right\|\right)}}, d\right], \tag{7}$$

where, *d* denotes the representative size of the crystal grain where dislocations move and the function Min[*] selects the smaller value from two arguments.

Continuum Mechanics-Based Crystal Plasticity Analysis of Yielding and Strain Hardening of Polycrystals

Polycrystal models with the mean grain diameter ranging from 0.2 to 30 μm are employed in this study. The models are homothetic to each other and consist of six crystal grains (Fig. 4). The proportion of the specimen is *W*:*H*:*D*=5:15:1. The material is assumed to be pure copper and there are twelve {111}<110> slip systems. Tensile load is applied to the specimen and slip deformation is analyzed by a crystal plasticity software code with the CRSS given by Eq. (2). Representative length scale *d* of each crystal grain in the model is calculated by the following equation,

$$\pi\left(\frac{d}{2}\right)^2 = (area\ of\ polygon) \quad . \tag{8}$$

Mean grain diameter $\bar{d}$ is close to the width of the specimen W and we assume $\bar{d} = W$. Grown-in dislocations are distributed uniformly on twelve slip systems. Material constants for Cu are used for the analyses and we assume $a = 0.3$, $c = 1$, D=0.5 nm, and $\beta = 1$ unless otherwise stated. We also assume isotropic latent hardening ($\Omega^{(ij)} \approx 1$, $i, j = 1,...12$).

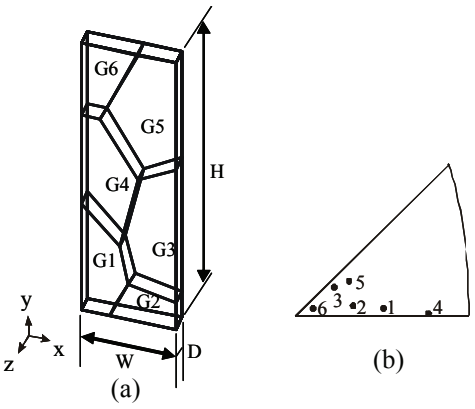

Fig.4 (a)Six-grained multicrystal model employed in this study, (b) crystal orientations.

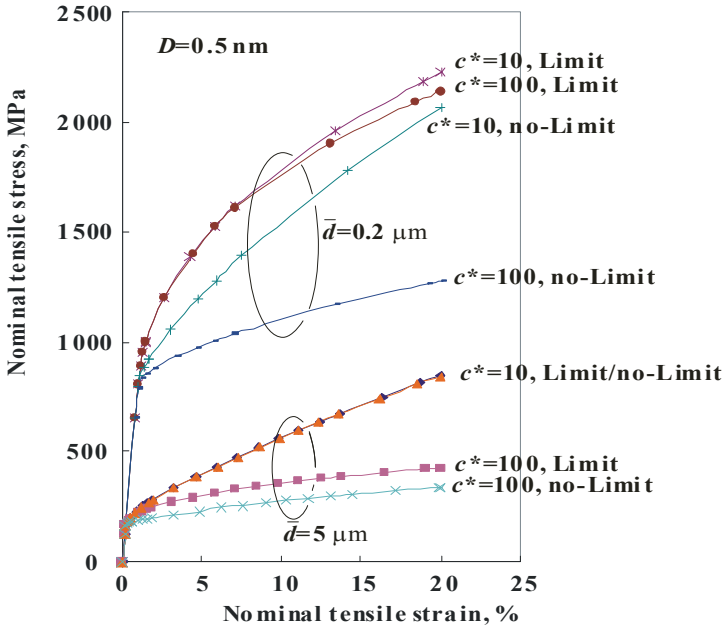

Fig.5 Stress-strain relations for polycrystal models obtained by the strain gradient crystal plasticity analyses. Limit and no-Limit denote the two models for dislocation mean free path given by Eqs. 4 and 7, respectively.

Results of the analyses for polycrystal specimens with the mean grain diameter 0.2 and 5 μm are summarized in Fig. 5. Some combination of c^* and the model for MFP are employed. Data annotated by **Limit** are calculated with the MFP model given by Eq. 7, while data annotated by **no-Limit** are obtained with the MFP model of Eq. 4.

Increase of yield stresses for specimens with $\bar{d} = 0.2\ \mu m$ compared to those for the specimens with $\bar{d} = 5\ \mu m$ is due to the difficulty in the dislocation emission from dislocation source, which is given by the third term in the right hand side of Eq. 2. When the mean grain diameter is 0.2 μm, limitation of the MFP by grain boundaries results in a notable increase in strain hardening ratios. This effect is more significant when c^* is larger. In contrast to these results, limitation of MFP in the specimens with $\bar{d} = 5\ \mu m$ is small. When the mean grain diameter is 0.2 μm, the strain hardening ratio just after the yield point is extremely large and the transition from the elastic to plastic region in the macroscopic stress-strain curve is ambiguous.

Comparison with experimental results

Stress-strain curves of ARB and ECAP processed Al polycrystals are compared with numerical results. Fig. 6 shows the experimental [9,10] and numerical results for normal-sized polycrystal specimen of 99% purity Al. The specimen used for the experiment was ARB processed for six cycles

and annealed for 1.8 ks at 773K. Mean sizes of crystal grains of the specimen were 9 and 9.5 μm in ND and RD directions, respectively. For the numerical analysis, polycrystal model shown in Fig. 4 is used. Mean grain diameter of the numerical specimen is 9 μm . Other input data used in the numerical analysis are; $\rho_0\big|_{total} = 1.2\times10^9 m^{-2}$, $\theta_0^{(n)} = 6.5\,MPa$, $c^* = 3$ and $D = 1$ nm.

Agreement of both curves is fine during the initial deformation period and then discrepancy in strain hardening property grows. The reason for the latter discrepancy is not clear but the model for the evolution of dislocations given by Eq. 3 is worth exploring in future study.

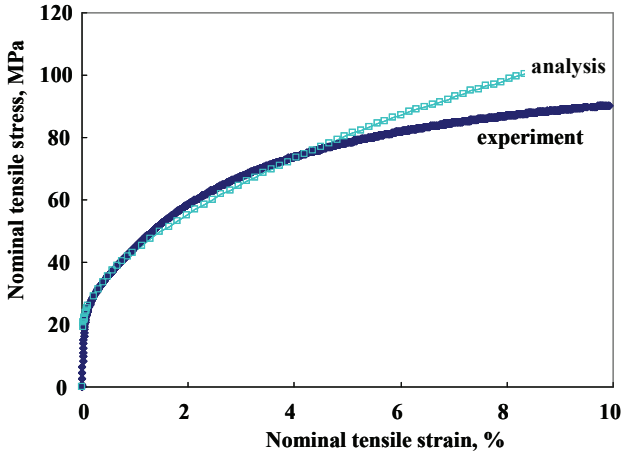

Fig.6 Comparison of stress-strain curves of polycrystals with normal-sized crystal grains. Experimental data were obtained by Tsuji and [9,10]. Mean grain diameter of the experimental and numerical specimen is about 9 μm .

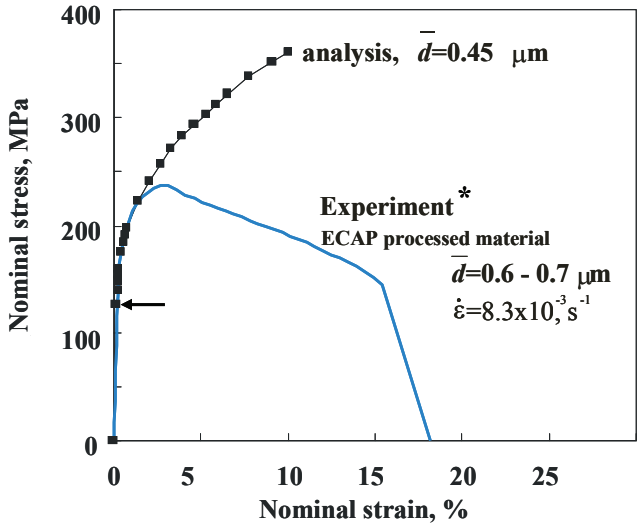

Fig.7 Comparison of stress-strain curves of fine grained polycrystals. Experimental data were obtained by Dvorak et al. [11]. Mean grain diameters of the experimental and numerical specimens are 0.6-0.7 and 0.45 μm , respectively.

Comparison of stress-strain curves for a fine-grained Al is shown in Fig. 7. Experimental result [11] was obtained from ECAP processed Al of 99% purity. The mean grain diameter was 0.6-0.7 μm and the tensile deformation was performed under nominal strain rate of 8.3×10^{-3}, s^{-1}. Numerical data are obtained by tensile deformation of the six-grained polycrystal model shown in Fig. 4. The mean

grain diameter of the numerical specimen is 0.45 μm . Onset of plastic slip in the numerical analysis is indicated by an arrow in the Fig. 7. Numerical and experimental data agree very well during the early stage of deformation and then the experimental data come to a lapse from high strain hardening character and after that, drop into unstable deformation stage. It is frequently mentioned that grain boundary can act as the sink for dislocations. The reason for the decrease of strain hardening rate observed in Fig. 7 is not clear yet, but one possible mechanism could be an accerelated extinction of dislocations at grain boundaries.

Summary

Strain gradient crystal plasticity theory with some models for the effect of dislocation-grain boundary interaction was described and macroscopic mechanical response of SPD-processed materials were predicted. Obtained results are summarized as follows.

1. Obstacle effect of dislocation emission from FR source was incorporated into the critical resolved shear stress of slip systems, and scale dependent character of yield stress of polycrystals were obtained.
2. Effect of grain boundaries on the mean free path of dislocations were introduced and this effect resulted in scale dependent strain hardening characteristics.
3. Stress-strain relationship for polycrystals predicted by the above mentioned models were compared to experimental data. Numerical and experimental results partly agreed and some discrepancies were observed.

Acknowledgment

The authors acknowledges that this work was performed under financial support from the Ministry of education, culture, sports, science and technology under Grant No. 18062001. Experimental data for stress-strain relations of SPD-processed materials were provided from Profs. Zenji Horita and Nobuyasu Tsuji. The authors also acknowledges their kind support.

References

[1] Fleck, N.A., Muller, G.M., Ashby, M.F. and Hutchinson, J.W.: Acta metall. mater., 42(1994), 475.
[2] Ohashi, T.: Solid mech. appl., vol. 115(2004), *Proc. IUTAM symposium*, Osaka, Kluwer, Dordrecht, eds., H. Kitagawa and Y. Shibutani, 97-106.
[3] Akasheh, F., Zbib, H. M. and Ohashi, T.: Phil. Mag., 87(2007), 1307-1326.
[4] Kuroda, M., Tvergaard, V. and Ohashi, T.: Modelling Simul. Mater. Sci. Eng., 15(2007), s13-s22.
[5] Ohashi, T., Kawamukai, M, and Zbib, H.M.: Int. J. Plasticity, vol. 23(2007), 897-914.
[6] Zbib, H.M., and Khraishi, T.A.: 2005, *Dislocation Dynamics, in: Handbook of materials modeling*, ed. Sidney Yip, pp1097-1114, Springer.
[7] Kocks, U.F.: Trans. ASME, J. Eng. Mater. Tech., 98**(**1976**)**, 76.
[8] Ohashi, T.: Int. J. Plasticity, 21(2005), 897-914.
[9] Tsuji, N.: J. of Nanoscience and Nanotechnology, 7(2007), 3765-3770.
[10] Kamikawa, N.: PhD Thesis, (2006) Osaka University
[11] Dvorak, J., Sklenicka, V. and Horita, Z.: Private communication.